Modal analysis by free vibration response only for discrete and continuous systems

Bor-Tsuen Wang*, Deng-Kai Cheng

Department of Mechanical Engineering, National Pingtung University of Science and Technology, Pingtung 91201, Taiwan

ARTICLE INFO

ABSTRACT

This work aims to develop the algorithm for modal analysis by free vibration response only (MAFVRO), in particular for the general or non-proportional viscous damping system model. If the structural displacement or acceleration response due to free vibration can be measured, the system response matrices, including the displacement, velocity and acceleration, can be obtained through numerical differential or integration methods. These response matrices can then be applied to the developed MAFVRO method to determine the structural modal parameters. The numerical differential and integration methods are introduced and adopted to establish the modal parameter prediction program for the non-proportional damping model of MAFVRO. This work also shows the applications of MAFVRO to the multiple degree-of-freedom (mdof) systems and the cantilever beam, respectively. Both the discrete and continuous systems are demonstrated for the feasibility of the MAFVRO algorithm. The developed method uses the free vibration output response only and can obtain the structural modal parameters successfully.

© 2011 Elsevier Ltd. All rights reserved.

1. Introduction

The knowledge of structural modal parameters is of great interest. Natural frequencies generally account for the structural mass and stiffness distributions. Mode shape patterns corresponding to the natural frequencies can be informative for structural design consideration or other monitoring purposes. Structural modal damping ratios are also of importance for theoretical simulations, since they are not theoretically available in general. In particular, experimentally extracted modal parameters can be useful for analytical model validation, structural design modification, response simulation for optimum design, force prediction, structural monitoring or damage detection. Experimental methods to identify the structural modal parameters are necessary.

In conventional experimental modal analysis (EMA) [1,2], the test structure is usually assumed to be at rest and without other external excitation during modal testing. For practical applications the test subject can be in operational conditions. The operational modal analysis (OMA) approach has drawn much attention. The operational conditions can be featured in several regimes, such as ambient excitation, natural source, free response and unknown or uncontrolled inputs. Therefore, output-only modal analysis (OOMA) is also termed and interested.

The selection of excitation forms and sensors is of importance in EMA. Wang [3] presented the theoretical formulation of generic frequency response functions (FRFs) for continuous systems and provided the theoretical base for applying various forms of actuators and sensors to structural modal testing. In EMA, the excitation should be controllable and

---

measurable. The impact hammer is frequently used as the actuator and the accelerometer as the sensor via a FFT analyzer to obtain the system FRFs between the excitation and the structural response. One can obtain structural modal parameters including natural frequencies, mode shapes and modal damping ratios using a curve-fitting process or modal parameter extraction methods. This traditional approach is categorized as input–output modal analysis. This work will focus on the output-only modal analysis for free vibration response only.

For the traditional EMA requiring FRFs, the operational modal analysis for frequency domain decomposition (FDD) methods [4,5], that have been developed and widely adopted for modal identification, starts from spectral density functions of system response. Cauberghe et al. [6] presented a combined experimental-operational modal analysis method to estimate the modal parameters by using the Fourier spectra of the outputs and known input. Magalhaes et al. [7] used the ambient vibration test (AVT) data for the modal identification of a cable-stayed bridge by Enhanced frequency domain decomposition (EFDD) and Stochastic Subspace Identification (SSI) methods. Gentile and Gallino [8] also applied the peak picking method and the EFDD techniques to extract the modal parameters from ambient vibration data for a suspension footbridge. For the above mentioned approaches, the fast Fourier transform (FFT) operation is generally required and causes the complexity for numerical operation of measured data in signal processing. This work mainly adopts the time domain method for requiring only free vibration response data and related matrix operations to determine structural modal parameters.

Another category of time domain modal identification approach is the autoregressive (AR) method. Moore et al. [9] presented an autoregressive moving average with exogenous excitation (ARMAX) time-domain parameter estimation algorithm to identify modal parameters of structures in the presence of significant measurement noise and unmeasured sources of periodic and random excitation. Larbi and Lardies [10] presented a time-domain procedure using the vector autoregressive moving-average (VARMA) process for identification of modal parameters of vibrating systems from multiple output data only based on the estimation of multivariate autoregressive (AR) coefficients using a maximum likelihood technique. Papakos and Fassois [11] presented a comprehensive autoregressive (AR) and linear multistage autoregressive moving average (LMS-ARMA) method for multi-channel identification of structures under unobservable excitation. The approach was demonstrated for modal identification of an aircraft skeleton structure.

Other special techniques in EMA are also developed. Devriendt and Guillaume [12] introduced an approach to identify modal parameters from output-only transmissibility measurements and demonstrated by means of an experimental test on a clamped beam. Devriendt and Guillaume [13] developed a transmissibility-based approach for output-only modal analysis where the unknown operational forces can be arbitrary. Parloo et al. [14] provided the estimation of the operational scaling factor by performing the experiment adding a controlled mass on the test structure so as to determine the normalized mode shape vector. Parloo et al. [15] further applied the idea to identify the force in operational condition during output-only modal analysis. Abdelghani et al. [16] presented the subspace-based damage detection and isolation algorithms for on-line structural monitoring of an airplane structure under unknown excitation. The modal results from the output-only subspace-based modal analysis are compared with those from the modal appropriation method [17], which is based on a pure sinusoidal excitation of the structure to obtain the modal parameters of one mode in each experiment.

For free vibration response modal analysis methods, Huang and Su [18] proposed an approach based on the continuous wavelet transform (CWT) to identify modal parameters of a linear system from its seismic response with the knowledge of source excitation. This method is applicable for the case of free decay response. Their approach employed the time invariance property and filtering ability of CWT to improve data processing efficiency. The approach was validated to obtain modal parameters for a three-story non-symmetric steel frame in a shaking table. Lardies [19] presented a time domain method from multi-output sensors only for modal parameter identification. The method used Cayley–Hamilton theorem to find a set of scalar parameters related to the modal properties of a vibrating system and required only knowledge of the covariance matrix of signals.

Wang and Cheng [20] proposed an algorithm of modal analysis from free vibration response only (MAFVRO). Their formulation is limited to the proportional viscous damping based on normal mode analysis. The natural frequencies and mode shape vectors for mdof systems can be successfully obtained. This work extends the MAFVRO to the general or non-proportional viscous damping cases. The complex mode analysis is adopted and thus the natural frequencies, complex mode shapes and modal damping ratios can be determined, simultaneously.

The MAFVRO method is inspired from Zhou and Chelidze [21] who used the free vibration response data and adopted smooth orthogonal decomposition (SOD) method to extract normal modes of discrete system requiring the prior knowledge of mass matrix. Feeny and Kappagantu [22] may be the first to discuss the modal analysis for structure in free vibration condition. They adopted proper orthogonal decomposition (POD) or so called Karhunen Loeve decomposition (KLD) to obtain mode shape vectors only. Han and Feeny [23] applied POD to obtain proper orthogonal mode (POM) that is the structural normal mode. The practical limitation is that the mass matrix must be proportional to the identity matrix. The MAFVRO algorithms presented in this work require no prior knowledge of system matrices in obtaining modal parameters, in particular the complex mode is also considered for the non-proportional damping model rather than the normal mode analysis in the proportional damping model [20].

This paper derives the complete MAFVRO formulation for both the proportional and non-proportional viscous damping models in Section 2 and considers both the displacement sensors and accelerometers applications, respectively, in Section 3. Section 4 introduces the development of MAFVRO application program in MATLAB software. Section 5 demonstrates the applications of the MAFVRO algorithm to the mdof discrete systems and the beam structure, i.e. a continuous system.

2. MAFVRO formulation

Consider an mdof vibration system with viscous damping. The general form of equation of motion can be expressed as follows:

$$\mathbf{M\ddot{x} + C\dot{x} + Kx = f}. \tag{1}$$

The initial conditions are:

$$\mathbf{x}(0) = \mathbf{x_0}, \tag{2}$$

$$\mathbf{\dot{x}}(0) = \mathbf{v_0}. \tag{3}$$

M, **C** and **K** are the $n \times n$ mass, damping and stiffness matrices of the mdof system, respectively, and n is the number of dofs for the system. $\mathbf{x}_0$ and $\mathbf{v}_0$ are the initial displacement and velocity vectors, respectively.

2.1. Proportional viscous damping model

For the proportional viscous damping, the following relation holds:

$$\mathbf{C} = \alpha\mathbf{M} + \beta\mathbf{K}, \tag{4}$$

where α and β are some constants. For normal mode analysis, let

$$\mathbf{x} = \mathbf{X}e^{i\omega t}. \tag{5}$$

By the substitution of Eq. (5) into Eq. (1) and the assumptions of $\mathbf{f} = \mathbf{0}$ and $\mathbf{C} = \mathbf{0}$, the generalized eigenvalues problem can be formulated:

$$\mathbf{KX} = \omega^2\mathbf{MX} \tag{6}$$

or

$$\mathbf{M^{-1}KX} = \omega^2\mathbf{X}. \tag{7}$$

By solving the above equation, n-pair of eigenvalues ω_r^2 and eigenvector $\mathbf{X_r}$ can be obtained. Physically, $\omega_r = 2\pi f_r$ is the rth natural frequency in rad/s, f_r is in Hz, and $\mathbf{X_r} = \boldsymbol{\phi_r}$ is its corresponding mode shape vector.

The following derivation is partly adopted from Wang and Cheng [20]. They showed the formulation to determine modal parameters from the free vibration response, i.e. $\mathbf{f} = 0$. For the proportional viscous damping model without the prescribed force, the system equation becomes

$$\mathbf{M\ddot{x}} + (\alpha\mathbf{M} + \beta\mathbf{K})\mathbf{\dot{x}} + \mathbf{Kx} = \mathbf{0}. \tag{8}$$

Rearrange the above equation

$$\mathbf{M}(\mathbf{\ddot{x}} + \alpha\mathbf{\dot{x}}) = -\mathbf{K}(\mathbf{x} + \beta\mathbf{\dot{x}}). \tag{9}$$

Then

$$\mathbf{M^{-1}K} = -(\mathbf{\ddot{x}} + \alpha\mathbf{\dot{x}})(\mathbf{x} + \beta\mathbf{\dot{x}})^{-1}. \tag{10}$$

By comparing Eqs. (10) and (7), one can conclude that if the system responses $\mathbf{x}$, $\mathbf{\dot{x}}$ and $\mathbf{\ddot{x}}$ are known, $\mathbf{M^{-1}K}$ can be formulated and used to solve for the eigenvalues and eigenvectors. The drawback of the formulation is the requirement of prior knowledge of constants α and β. For the proportional viscous damping model, i.e. the normal modes of the system, the natural frequencies $\hat{\omega}_r = 2\pi\hat{f}_r$ and mode shape vectors $\boldsymbol{\hat{\phi}_r}$ can be obtained, in particular $\boldsymbol{\hat{\phi}_r}$ is real. The symbol ^ denotes the solutions from the proportional model.

Consider the system displacement response matrix as follows:

$$\mathbf{X}(t) = [X]_{N_k \times n} = \begin{bmatrix} x_{1,k} & x_{2,k} & \cdots & x_{n,k} \\ x_{1,k+1} & x_{2,k+1} & \cdots & x_{n,k+1} \\ \vdots & \vdots & \ddots & \vdots \\ x_{1,k+N_k-1} & x_{2,k+N_k-1} & \cdots & x_{n,k+N_k-1} \end{bmatrix} = \left[\begin{Bmatrix} x_{1,k} \\ x_{2,k} \\ \vdots \\ x_{n,k} \end{Bmatrix} \begin{Bmatrix} x_{1,k+1} \\ x_{2,k+1} \\ \vdots \\ x_{n,k+1} \end{Bmatrix} \cdots \begin{Bmatrix} x_{1,k+N_k-1} \\ x_{2,k+N_k-1} \\ \vdots \\ x_{n,k+N_k-1} \end{Bmatrix} \right]^T$$

$$= [\{x\}_k \{x\}_{k+1} \cdots \{x\}_{k+N_k-1}]^T, \tag{11}$$

where $x_{r,k} = x_r(t_k)$ denotes the displacement of the rth dof at time t_k as depicted in Fig. 1. k is the starting point, and N_k is the total number of points adopted for MAFVRO algorithm. [ ] and { } denote the matrix and vector, respectively. The superscript T denotes the transpose operation on the matrix. Similarly, the system velocity and acceleration response
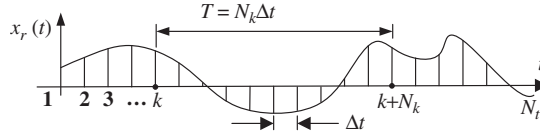
Fig. 1. Diagram for the time domain response.

matrix can also be defined

$$\dot{\mathbf{X}} = [\dot{X}] = [\{\dot{x}\}_k\{\dot{x}\}_{k+1}\cdots\{\dot{x}\}_{k+N_k-1}]^{\mathrm{T}},$$ (12)

$$\ddot{\mathbf{X}} = [\ddot{X}] = [\{\ddot{x}\}_k\{\ddot{x}\}_{k+1}\cdots\{\ddot{x}\}_{k+N_k-1}]^{\mathrm{T}}.$$ (13)

Eq. (10) can then be rewritten as follows:

$$\mathbf{M}^{-1}\mathbf{K} = -(\ddot{\mathbf{X}}^{\mathbf{T}}+\alpha\dot{\mathbf{X}}^{\mathbf{T}})(\beta\dot{\mathbf{X}}^{\mathbf{T}}+\mathbf{X}^{\mathbf{T}})^{-1}.$$ (14)

The measurement and derivation of those response matrices will be discussed in Section 3.

2.2. Non-proportional viscous damping model

For the general or non-proportional viscous damping, the following equilibrium equation is invoked:

$$\mathbf{M}\dot{\mathbf{x}}-\mathbf{M}\dot{\mathbf{x}} = 0.$$ (15)

By combining Eqs. (1) and (15), the system equation can be rewritten as follows:

$$\mathbf{A}\dot{\mathbf{y}}+\mathbf{B}\mathbf{y} = \mathbf{P},$$ (16)

where

$$\mathbf{A} = \begin{bmatrix} \mathbf{0} & \mathbf{M} \\ \mathbf{M} & \mathbf{C} \end{bmatrix}, \quad \mathbf{B} = \begin{bmatrix} -\mathbf{M} & \mathbf{0} \\ \mathbf{0} & \mathbf{K} \end{bmatrix}, \quad \mathbf{y} = \begin{Bmatrix} \dot{\mathbf{x}} \\ \mathbf{x} \end{Bmatrix}, \quad \mathbf{P} = \begin{Bmatrix} \mathbf{0} \\ \mathbf{f} \end{Bmatrix}.$$ (17)

Let

$$\mathbf{y} = \mathbf{Y}e^{\lambda t}.$$ (18)

By substitution of Eq. (18) into Eq. (16) and the assumption of zero external force vectors $\mathbf{f}=0$, i.e. $\mathbf{P}=0$, the eigenvalue problem can be formulated as follows:

$$\mathbf{B}\mathbf{Y} = -\lambda\mathbf{A}\mathbf{Y}$$ (19)

or

$$(-\mathbf{A}^{-1}\mathbf{B})\mathbf{Y} = \lambda\mathbf{Y}.$$ (20)

By solving the above equation, $2n$-pair of complex conjugate eigenvalues and their corresponding eigenvectors can be obtained:

$$\begin{cases} \lambda_r \rightarrow \mathbf{Y}_r \\ \lambda_r^* \rightarrow \mathbf{Y}_r^*, \end{cases} \quad r = 1,2,\dots,n,$$ (21)

where

$$\begin{matrix} \lambda_r \\ \lambda_r^* \end{matrix} = R_e \pm iI_m = -\overline{\zeta}_r\overline{\omega}_r \pm i\overline{\omega}_r\sqrt{1-\overline{\zeta}_r^2}.$$ (22)

The equivalent natural frequency and modal damping ratio can be determined:

$$\overline{\omega}_r = \sqrt{R_e^2+I_m^2},$$ (23)

$$\overline{\zeta}_r = \frac{-R_e}{\sqrt{R_e^2+I_m^2}}$$ (24)

and

$$\mathbf{Y}_r = \begin{Bmatrix} \dot{\overline{\mathbf{X}}}_r \\ \overline{\mathbf{X}}_r \end{Bmatrix}, \quad \mathbf{Y}_r^* = \begin{Bmatrix} \dot{\overline{\mathbf{X}}}_r^* \\ \overline{\mathbf{X}}_r^* \end{Bmatrix}.$$ (25)

where $\overline{\omega}_r = 2\pi \overline{f}_r$, $\overline{\zeta}_r$ and $\overline{\boldsymbol{\phi}}_{\mathbf{r}} = \overline{\mathbf{X}}_{\mathbf{r}}$ are the rth natural frequency, modal damping ratio and displacement mode shape vector, respectively. The bar symbol is to denote the solutions from the complex mode analysis, in particular for the non-proportional viscous damping.

Similar to the derivation of the proportional viscous damping model for MAFVRO, this work is mainly to extend the MAFVRO for the non-proportional viscous damping model. The system equation in Eq. (16) without the prescribed force, i.e. $\mathbf{P} = 0$, is as follows:

$$\mathbf{A}\dot{\mathbf{y}} + \mathbf{B}\mathbf{y} = \mathbf{0}. \tag{26}$$

One can obtain

$$-\mathbf{A}^{-1}\mathbf{B} = \dot{\mathbf{y}}\mathbf{y}^{-1} = \begin{Bmatrix} \ddot{\mathbf{x}} \\ \dot{\mathbf{x}} \end{Bmatrix} \begin{Bmatrix} \dot{\mathbf{x}} \\ \mathbf{x} \end{Bmatrix}^{-1}. \tag{27}$$

From the definition of the system displacement, velocity and acceleration response matrices as shown in Eqs. (11)–(13), the above equation becomes

$$-\mathbf{A}^{-1}\mathbf{B} = \begin{Bmatrix} \ddot{\mathbf{X}}^{\mathrm{T}} \\ \dot{\mathbf{X}}^{\mathrm{T}} \end{Bmatrix} \begin{Bmatrix} \dot{\mathbf{X}}^{\mathrm{T}} \\ \mathbf{X}^{\mathrm{T}} \end{Bmatrix}^{-1}. \tag{28}$$

By comparing Eqs. (20) and (28), one can see that if the system response matrices are known, $-\mathbf{A}^{-1}\mathbf{B}$ can be formulated and used to solve the eigenvalues and eigenvectors. Therefore, the system modal parameters as shown in Eqs. (23)–(25) can be obtained. This approach is the main idea of MAFVRO for the non-proportional viscous damping.

Note that the MAFVRO algorithms for both proportional and non-proportional viscous damping mdof systems are formulated. Only the rth natural frequency ($\hat{\omega}_r$) and its corresponding mode shape ($\hat{\boldsymbol{\phi}}_{\mathbf{r}}$) can be obtained for the proportional viscous damping model and the normal mode analysis is assumed, i.e. $\hat{\boldsymbol{\phi}}_{\mathbf{r}}$ is the real mode. For the non-proportional viscous damping model, the complex mode analysis is adopted, so the equivalent natural frequency ($\overline{\omega}_r$) and modal damping ratio ($\overline{\zeta}_r$) can be obtained from Eqs. (23) and (24). The mode shape vector ($\overline{\boldsymbol{\phi}}_{\mathbf{r}}$) is essentially complex. The novelty of MAFVRO for the non-proportional viscous damping in this work is that only the system transient response, such as the displacement or acceleration, is required to formulate the response matrices as described in Eqs. (11)–(13) and to obtain $-\mathbf{A}^{-1}\mathbf{B}$ as shown in Eq. (28). The modal parameters of the system can be predicted as discussed. Section 3 will show the formulation of system response matrices for different types of sensors.

It is also noted that the developed MAFVRO approach for mdof systems can be applied to a continuous structure as well. If the structure is divided into m measurement points, and single axial measurement is applied at each point, then the number of measurement points m can be considered as the dofs of the equivalent lumped mass system, i.e. the number of dofs becomes $n = m$. The formulation of MAFVRO can still be valid for continuous systems. The case study for the beam structure in Section 5 will be shown to demonstrate the application of MAFVRO to the continuous system.

3. Different sensor applications

Section 2 shows the theoretical formulation of the MAFVRO algorithm for both the proportional and non-proportional viscous damping models. The requirement of the algorithm is to provide the system displacement, velocity and acceleration response matrices due to free vibration. Wang and Cheng [20] illustrated the use of displacement sensor for the proportional viscous damping model of MAFVRO. This section will show the implement for selecting different sensors, in particular for the accelerometer that is frequently used.

If the displacement sensor is used to measure the system displacement response, $x_r(t_k) = x_{r,k}$, as illustrated in Fig. 1, the velocity and acceleration can be determined by finite difference method. Table 1 shows the formulas to evaluate the velocity and acceleration. Wang and Cheng [20] showed the matrix operations on response matrices, which are omitted here for brevity. The high-order formula can provide more accurate results as desired.

If the accelerometer is used, the acceleration at the rth dof $\ddot{x}_r(t_k) = \ddot{x}_{r,k}$ can be measured. Table 2 shows the numerical formulas to evaluate the velocity and displacement, respectively. Therefore, both Eqs. (14) and (28), for the proportional

Table 1
Numerical methods to evaluate velocity and acceleration from displacement [19].

Method	Velocity	Acceleration
First-order backward formula	$v_{r,k} = \dot{x}_{r,k} = \frac{1}{\Delta t}(x_{r,k} - x_{r,k-1})$	$a_{r,k} = \ddot{x}_{r,k} = \frac{1}{\Delta t}(v_{r,k} - v_{r,k-1})$
Second-order backward formula	$v_{r,k} = \dot{x}_{r,k} = \frac{1}{2\Delta t}(3x_{r,k} - 4x_{r,k-1} + x_{r,k-2})$	$a_{r,k} = \ddot{x}_{r,k} = \frac{1}{2\cdot\Delta t}(3v_{r,k} - 4v_{r,k-1} + v_{r,k-2})$
First-order central formula	$v_{r,k} = \dot{x}_{r,k} = \frac{1}{2\Delta t}(x_{r,k+1} - x_{r,k-1})$	$a_{r,k} = \ddot{x}_{r,k} = \frac{1}{2\Delta t}(v_{r,k+1} - v_{r,k-1})$
Second-order central formula	$v_{r,k} = \dot{x}_{r,k} = \frac{1}{12\Delta t}(-x_{r,k+2} + 8x_{r,k+1} - 8x_{r,k-1} + x_{r,k-2})$	$a_{r,k} = \ddot{x}_{r,k} = \frac{1}{12\Delta t}(-v_{r,k+2} + 8v_{r,k+1} - 8v_{r,k-1} + v_{r,k-2})$

Table 2
Numerical methods to evaluate velocity and displacement from acceleration.

Method	Velocity	Displacement
Mid-point rule	$v_{r,k} = v_{r,k-2} + 2\Delta t\, a_{r,k-1}$	$x_{r,k} = x_{r,k-2} + 2\Delta t\, v_{r,k-1}$
Trapezoid rule	$v_{r,k} = v_{r,k-1} + \frac{\Delta t}{2}(a_{r,k-1} + a_{r,k})$	$x_{r,k} = x_{r,k-1} + \frac{\Delta t}{2}(v_{r,k-1} + v_{r,k})$
Simpson's rule	$v_{r,k} = v_{r,k-2} + \frac{\Delta t}{3}(a_{r,k-2} + 4a_{r,k-1} + a_{r,k})$	$x_{r,k} = x_{r,k-2} + \frac{\Delta t}{3}(v_{r,k-2} + 4v_{r,k-1} + v_{r,k})$

and non-proportional viscous damping models of the MAFVRO algorithms, respectively, can be obtained from the free vibration response and solved for modal parameters. For example, if Simpson's rule is adopted to obtain the velocity and displacement from the acceleration as shown in Table 2, the minimum start number is $k=5$ for the displacement response matrix shown in Eq. (11) because two previous data points are required for each numerical integration operation.

4. Implementation of MAFVRO

This section introduces the development of MATLAB program to implement the MAFVRO algorithm. Fig. 2(a) shows the solution flow chart for the MAFVRO application program. The steps in the program are summarized as follows:

(1) Define the program parameters for the MAFVRO algorithm. Set up the start number of time data k and total number of time data N_k to be processed as revealed in Fig. 1.
(2) Select the analysis modes. Either the experiment or simulation can be selected. For the experiment, the measured data, either the displacement or acceleration response, due to the free vibration should be provided. For simulation, the free vibration simulation procedure is shown in Fig. 2(b). To perform the response simulation, define the system matrices first, as well as the initial conditions. Then, choose the time interval Δt, i.e. the sampling frequency is as follows:

$$f_s = \frac{1}{\Delta t}. \tag{29}$$

Next, define the noise ratio (NR), which is the ratio of noise and the maximum response amplitude for emulating the measured response containing noise as follows:

$$x_r(t_k) = \text{MAX}(|x_r(t_k)|) \cdot \text{NR} \cdot \text{RAN} + x_r(t_k), \tag{30}$$

where RAN is the normally distributed random number between -1 and 1; $\text{MAX}(|x_r(t_k)|)$ is the maximum displacement in simulation. Finally, the response model for either the proportional or non-proportional viscous damping can be specified and solved for both the theoretical modal analysis and transient response analysis. The displacement response can then be obtained and used for the MAFVRO algorithm applications. The simulated acceleration can also be obtained such as by the Simpson's rule as shown in Table 2.
(3) Define the type of sensor. Typical sensors including the displacement sensor and accelerometer can be specified.
(4) Obtain the system free vibration response matrices, including the displacement, velocity and acceleration as shown in Eqs. (11)–(13). Different numerical formula can be chosen for those differential and integration methods as shown in Tables 1 and 2.
(5) Start MAFVRO main program. To obtain the modal parameters from the free vibration response by choosing either the proportional or non-proportional viscous damping model of the MAFVRO algorithms as revealed in Fig. 2(c). It is noted here that only the rth natural frequency ($\hat{\omega}_r$) and its corresponding mode shape ($\hat{\boldsymbol{\phi}}_{\mathbf{r}}$) can be obtained for the proportional viscous damping model, because the normal mode analysis is assumed, i.e. $\hat{\boldsymbol{\phi}}_{\mathbf{r}}$ is the real mode. For the non-proportional viscous damping model, the complex mode analysis is adopted, so the equivalent natural frequency ($\overline{\omega}_r$) and modal damping ratio ($\overline{\zeta}_r$) can be obtained from Eqs. (23) and (24). The mode shape vector ($\overline{\boldsymbol{\phi}}_{\mathbf{r}}$) is essentially complex.
(6) Results comparison. The predicted modal parameters from the MAFVRO algorithm can be compared with those from the theoretical modal analysis (TMA) or the conventional experimental modal analysis (EMA). The prediction error for each modal frequency is defined as follows:

$$\varepsilon_r = \frac{\hat{f}_r - f_r}{f_r} \times 100\%. \tag{31}$$

The damping ratio prediction error is also defined similarly. In particular, the modal assurance criterion (MAC) value between two vectors is used to evaluate the prediction effectiveness for mode shapes and given as follows:

$$\text{MAC}(\hat{\boldsymbol{\phi}}_r, \boldsymbol{\phi}_s) = \frac{|\hat{\boldsymbol{\phi}}_r^{\mathsf{T}} \boldsymbol{\phi}_s|^2}{(\hat{\boldsymbol{\phi}}_r^{\mathsf{T}} \hat{\boldsymbol{\phi}}_r^*)(\boldsymbol{\phi}_s^{\mathsf{T}} \boldsymbol{\phi}_s^*)}, \quad r = 1,2,\dots,n, \quad s = 1,2,\dots,n. \tag{32}$$

If MAC($\hat{\phi}_r,\phi_s$)=1, the two mode shape vectors are perfectly proportional. For MAC($\hat{\phi}_r,\phi_s$)=0, the two mode shape vectors are truly orthogonal.

5. Results and discussions

This section will employ the developed MAFVRO algorithms for both the proportional and non-proportional viscous damping models to obtain the structural modal parameters via simulation data. Sections 5.1 and 5.2 show the applications of MAFVRO to the mdof systems and the beam structure, respectively.
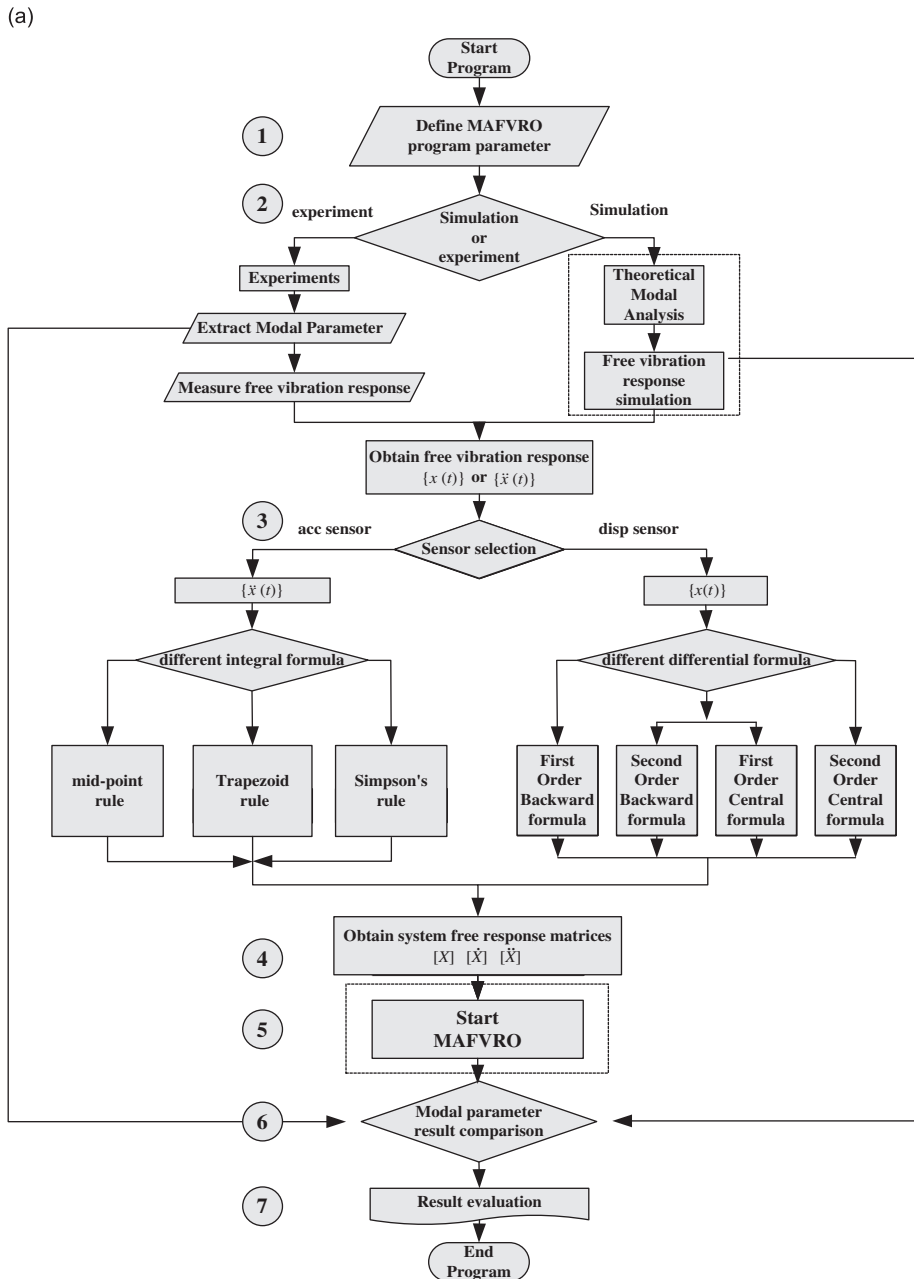

Fig. 2. Solution flow chart for MAFVRO application program: (a) application procedure; (b) response simulation procedure; and (c) MAFVRO main program.

(b)

(c)

Fig. 2. (continued)

5.1. mdof System application
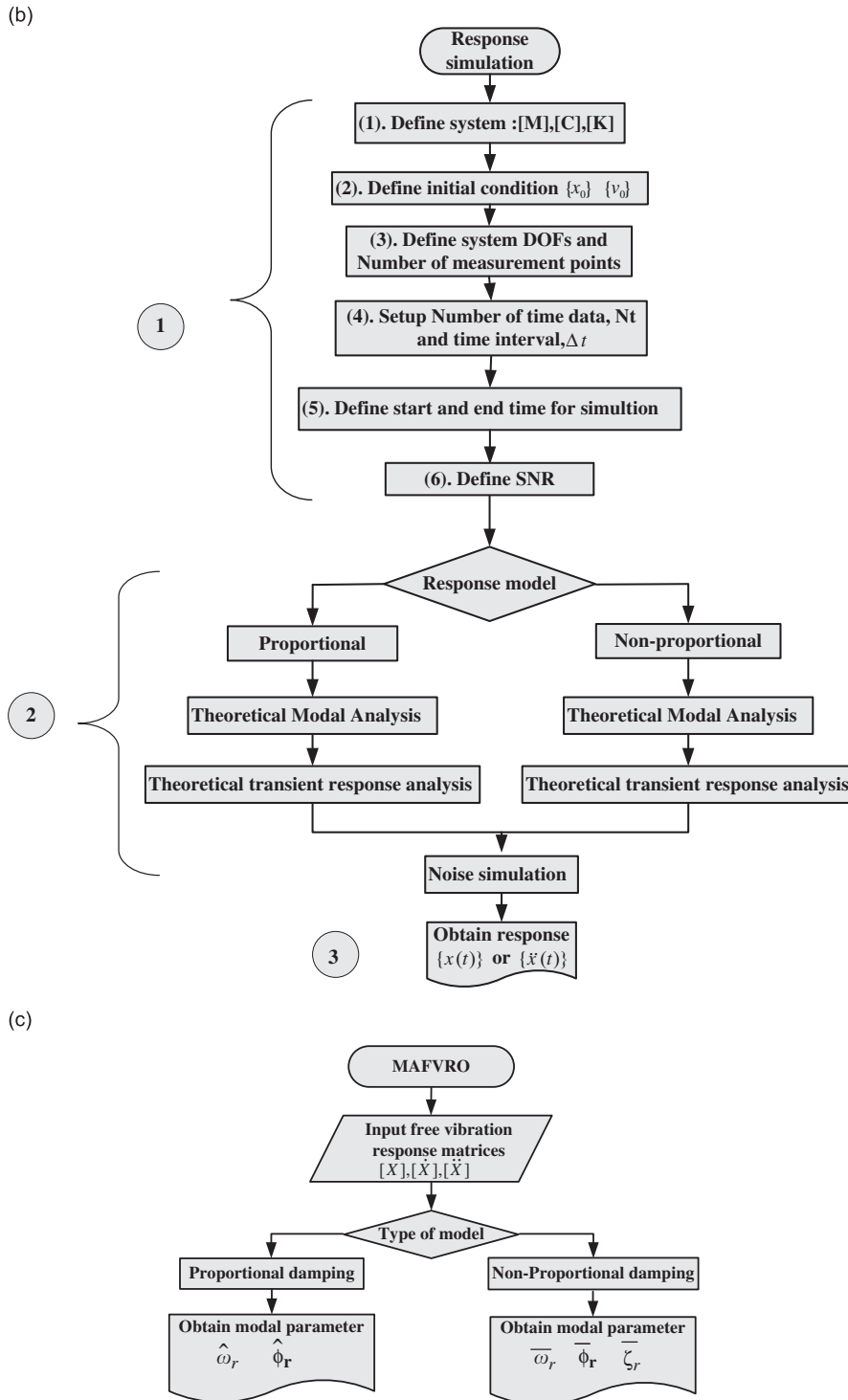
Fig. 3 shows the diagram of a n-dof system model. Table 3 summarizes the system parameters and the damping matrix **C** has the similar form to the stiffness matrix **K**, where $m_i = 1$ kg and $k_i = 1,000,000$ N/m. For the proportional viscous damping system model, the constants defined in Eq. (4) are assumed as $\alpha = 0.00001$ and $\beta = 0.00001$. Table 4 shows natural
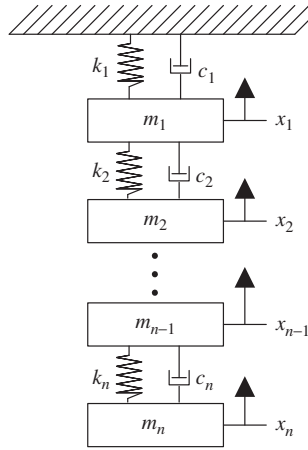
Fig. 3. n-dof System model.

Table 3
System parameters for mdof system.

System	n dofs
M	$\begin{bmatrix} m_1 & 0 & 0 & \cdots & 0 \\ 0 & m_2 & 0 & \cdots & 0 \\ 0 & 0 & m_3 & \ddots & \vdots \\ \vdots & \vdots & \ddots & \ddots & 0 \\ 0 & 0 & \cdots & 0 & m_n \end{bmatrix}_{n \times n}$
K	$\begin{bmatrix} (k_1+k_2) & -k_2 & \cdots & 0 & 0 \\ -k_2 & (k_2+k_3) & \cdots & 0 & 0 \\ \vdots & \vdots & \ddots & \ddots & \vdots \\ \vdots & \vdots & & \ddots & (k_{n-1}+k_n) & -k_n \\ 0 & 0 & \cdots & -k_n & k_n \end{bmatrix}_{n \times n}$
I.C.	$\mathbf{x_0^T} = [1;1;...;1]_{n \times 1}$ $\mathbf{v_0^T} = [0; 0; ... ; 0]_{n \times 1}$

Table 4
Normal mode analysis for different dofs in proportional damping systems, $m_i=1$ (kg), $k_i=1{,}000{,}000$ (N/m), $i=1,2,...,n$, $\alpha=0.00001$, $\beta=0.00001$.

dofs	Mode									
	1	2	3	4	5	6	7	8	9	10
(a) Natural frequency (Hz)										
3	70.830	198.463	286.787	–	–	–	–	–	–	–
4	55.273	159.155	243.840	299.113	–	–	–	–	–	–
5	45.300	132.231	208.449	267.779	305.416	–	–	–	–	–
6	38.368	112.874	180.821	238.258	281.849	309.060	–	–	–	–
7	33.272	98.363	159.155	212.991	257.518	290.791	311.354	–	–	–
8	29.369	87.109	141.883	191.825	235.234	270.633	296.815	312.89	–	–
9	26.285	78.140	127.864	174.099	215.585	251.191	279.945	301.063	313.969	–
10	23.787	70.830	116.291	159.154	198.463	233.337	263.000	286.787	304.168	314.754
(b) Damping ratio (%)										
3	0.2225	0.6235	0.9010	–	–	–	–	–	–	–
4	0.1736	0.5000	0.7660	0.9397	–	–	–	–	–	–
5	0.1423	0.4154	0.6549	0.8413	0.9595	–	–	–	–	–
6	0.1205	0.3546	0.5681	0.7485	0.8855	0.9709	–	–	–	–
7	0.1045	0.3090	0.5000	0.6691	0.8090	0.9135	0.9781	–	–	–
8	0.0923	0.2737	0.4457	0.6026	0.7390	0.8502	0.9325	0.9830	–	–
9	0.0826	0.2455	0.4017	0.5469	0.6773	0.7891	0.8795	0.9458	0.9864	–
10	0.0747	0.2225	0.3653	0.5000	0.6235	0.7331	0.8262	0.9010	0.9556	0.9888

Table 5
Complex mode analysis for different dofs in non-proportional damping systems, $m_i=1$ (kg), $k_i=1,000,000$ (N/m), $i=1,2,\ldots,n$, $c_1=20$ (N s/m) $c_i=0$.

dofs	Mode									
	1	2	3	4	5	6	7	8	9	10
(a) Natural frequency (Hz)										
3	70.831	198.465	286.780	–	–	–	–	–	–	–
4	55.274	159.158	243.837	299.107	–	–	–	–	–	–
5	45.300	132.233	208.450	267.774	305.412	–	–	–	–	–
6	38.368	112.870	180.823	238.257	281.844	309.057	–	–	–	–
7	33.272	98.364	159.157	212.991	257.515	290.786	311.352	–	–	–
8	29.370	87.110	141.885	191.826	235.233	270.628	296.811	312.888	–	–
9	26.285	78.141	127.865	174.101	215.586	251.189	279.941	301.059	313.967	–
10	23.787	70.831	116.292	159.156	198.464	233.337	262.997	286.783	304.165	314.753
(b) Damping ratio (%)										
3	0.2417	0.4356	0.1938	–	–	–	–	–	–	–
4	0.1497	0.3333	0.2814	0.0977	–	–	–	–	–	–
5	0.1014	0.2500	0.2721	0.1788	0.0554	–	–	–	–	–
6	0.0731	0.1908	0.2368	0.2026	0.1177	0.0342	–	–	–	–
7	0.0551	0.1491	0.2000	0.1971	0.1491	0.0806	0.0225	–	–	–
8	0.0431	0.1191	0.1681	0.1806	0.1579	0.1109	0.0572	0.0156	–	–
9	0.0345	0.0971	0.1418	0.1614	0.1544	0.1254	0.0839	0.0420	0.0112	–
10	0.0283	0.0806	0.1206	0.1429	0.1452	0.1292	0.0999	0.0646	0.0316	0.0084

frequencies and damping ratios determined by normal mode analysis for systems with different numbers of dofs. For the non-proportional viscous damping system model, only $c_1=20$(N s/m) and else $c_i=0$. Table 5 reveals natural frequencies and damping ratios, as shown in Eqs. (23) and (24), respectively, determined by complex mode analysis for different dofs systems. One can observe that there is a slight difference for natural frequencies between the proportional and non-proportional viscous damping models, while the damping ratios are quite different for different damping models and their assumptions. The following case studies of different dofs systems for both the proportional and non-proportional viscous damping system models are adopted accordingly.

For the adoption of MAFVRO algorithms to obtain modal parameters via either the proportional or non-proportional damping method, the system response matrices, including displacement, velocity and acceleration, must be formulated first. In this paper unless noted, the second-order central formula is adopted to evaluate the velocity and acceleration for using the displacement sensors to measure the response. For the use of accelerometers, the Simpson's rule is adopted to numerically obtain the velocity and displacement response from the acceleration.

Wang and Cheng [20] showed the system parameter effects of MAFVRO algorithm, including the starting data point k and total number of time data N_k as well as the sampling frequency f_s, for using the displacement sensor by the proportional viscous damping MAFVRO method. Wang and Cheng [20] showed the prediction of natural frequencies are exactly the same for different N_k and k, respectively, because the formulation of system response matrices as revealed in Eqs. (11)–(13) are nearly exact solution. Therefore, different N_k and k can be flexibly chosen to formulate system matrices and result in good predictions of natural frequencies and mode shapes. This work will mainly show the prediction by the non-proportional viscous damping MAFVRO method and compare the performance between both models. The commonly used accelerometers in experimental measurements for the MAFVRO application are shown additionally in this work.

Table 6 shows the prediction of modal parameters for the 10 dofs system with the non-proportional viscous damping effect by using displacement sensor and adopting the non-proportional MAFVRO method. Table 6(a) reveals the effect of different number of data points (N_k) for starting data point $k=5$ on the modal parameter prediction. Both predicted natural frequency errors ε_i and damping ratio errors are quite small and reveal the same for $N_k > 100$, while the MACs for the predicted mode shapes in comparison to the theoretical ones are equal to one for each mode, i.e. the perfect prediction for mode shapes. Table 6(b) is the results for different starting data points (k), when $N_k=100$. The prediction of modal parameters is also very good. The merit of MAFVRO method is that if the system response matrices can be formulated as accurately as possible, the prediction of modal parameters will be almost exact solutions. The selection of starting data point (k) and the number of data points (N_k) can be flexibly chosen and result in very good prediction of modal parameters by the MAFVRO method.

Table 7 shows the minimum sampling frequency for different numerical methods via different sensor applications by the non-proportional viscous damping model of the MAFVRO algorithm. One can see that the natural frequency predictions are within 2% errors for the second central formula in the displacement sensor application, when f_s is 2200 Hz, i.e. the frequency ratio between the sampling frequency and the highest modal frequency is about 7.12. For the accelerometer application, the use of Simpson's rule can obtain accurate predictions if $f_s=3800$ Hz, i.e. the frequency ratio about 12.23. The higher order of numerical methods used in obtaining the response matrices will result in better accuracy and require the smaller sampling frequency. Table 7 suggests the required sampling frequencies as the guideline for practical applications in using displacement sensors and accelerometers.

Table 6
Prediction of modal parameters for the non-proportional damping system model by using displacement sensor, adopting the non-proportional MAFVRO model, MAFVRO parameters: $f_s = 6000$ Hz, NR $= 0$(%).

(a) *Different number of data points* (N_k), *k*=5

N_k	Mode	1	2	3	4	5	6	7	8	9	10
50	ε_i (%)	0.0079	−0.0021	1.7e−005	−0.0041	−0.0052	−0.0148	−0.0184	−0.0264	−0.0334	−0.0388
60		0.0001	−1.6e−005	−0.0008	−0.0026	−0.0062	−0.0118	−0.0189	−0.0267	−0.0338	−0.0388
75		−3.5e−006	−0.0001	−0.0007	−0.0026	−0.0062	−0.0118	−0.0189	−0.0267	−0.0338	−0.0388
100		−1.3e−006	−0.0001	−0.0007	−0.0026	−0.0062	−0.0118	−0.0189	−0.0267	−0.0338	−0.0388
200		−1.3e−006	−0.0001	−0.0007	−0.0026	−0.0062	−0.0118	−0.0189	−0.0267	−0.0338	−0.0388
300		−1.3e−006	−0.0001	−0.0007	−0.0026	−0.0062	−0.0118	−0.0189	−0.0267	−0.0338	−0.0388
400		−1.3e−006	−0.0001	−0.0007	−0.0026	−0.0062	−0.0118	−0.0189	−0.0267	−0.0338	−0.0388
500		−1.3e−006	−0.0001	−0.0007	−0.0026	−0.0062	−0.0118	−0.0189	−0.0267	−0.0338	−0.0388
600		−1.3e−006	−0.0001	−0.0007	−0.0026	−0.0062	−0.0118	−0.0189	−0.0267	−0.0338	−0.0388
1000		−1.3e−006	−0.0001	−0.0007	−0.0026	−0.0062	−0.0118	−0.0189	−0.0267	−0.0338	−0.0388
50	Damping error (%)	3.1436	0.1552	0.1131	−0.0147	−0.2143	−0.2593	−0.0487	−0.1533	−0.3184	−0.978
60		0.0307	−0.0139	−0.0038	−0.0113	−0.0266	−0.0469	−0.0761	−0.1031	−0.1365	−0.1537
75		−0.0005	−0.0003	−0.0029	−0.0103	−0.0248	−0.047	−0.0753	−0.1062	−0.1345	−0.1543
100		−4.4e−006	−0.0004	−0.0029	−0.0103	−0.0247	−0.047	−0.0753	−0.1062	−0.1344	−0.1543
200		−5.1e−006	−0.0004	−0.0029	−0.0103	−0.0247	−0.047	−0.0753	−0.1062	−0.1344	−0.1543
300		−5.1e−006	−0.0004	−0.0029	−0.0103	−0.0247	−0.047	−0.0753	−0.1062	−0.1344	−0.1543
400		−5.1e−006	−0.0004	−0.0029	−0.0103	−0.0247	−0.047	−0.0753	−0.1062	−0.1344	−0.1543
500		−5.1e−006	−0.0004	−0.0029	−0.0103	−0.0247	−0.047	−0.0753	−0.1062	−0.1344	−0.1543
600		−5.1e−006	−0.0004	−0.0029	−0.0103	−0.0247	−0.047	−0.0753	−0.1062	−0.1344	−0.1543
1000		−5.1e−006	−0.0004	−0.0029	−0.0103	−0.0247	−0.047	−0.0753	−0.1062	−0.1344	−0.1543
50	MAC	1	1	1	1	1	1	1	1	1	1
100		1	1	1	1	1	1	1	1	1	1
200		1	1	1	1	1	1	1	1	1	1
300		1	1	1	1	1	1	1	1	1	1
400		1	1	1	1	1	1	1	1	1	1
500		1	1	1	1	1	1	1	1	1	1
600		1	1	1	1	1	1	1	1	1	1
1000		1	1	1	1	1	1	1	1	1	1

(b) *Different starting data points* (*k*), N_k=100

k	Mode	1	2	3	4	5	6	7	8	9	10
5	ε_i (%)	−1.3e−006	−0.0001	−0.0007	−0.0026	−0.0062	−0.0118	−0.0189	−0.0267	−0.0338	−0.0388
50		−1.3e−006	−0.0001	−0.0007	−0.0026	−0.0062	−0.0118	−0.0189	−0.0267	−0.0338	−0.0388
100		−1.3e−006	−0.0001	−0.0007	−0.0026	−0.0062	−0.0118	−0.0189	−0.0267	−0.0338	−0.0388
200		−1.3e−006	−0.0001	−0.0007	−0.0026	−0.0062	−0.0118	−0.0189	−0.0267	−0.0338	−0.0388
300		−1.3e−006	−0.0001	−0.0007	−0.0026	−0.0062	−0.0118	−0.0189	−0.0267	−0.0338	−0.0388
400		−1.3e−006	−0.0001	−0.0007	−0.0026	−0.0062	−0.0118	−0.0189	−0.0267	−0.0338	−0.0388
500		−1.3e−006	−0.0001	−0.0007	−0.0026	−0.0062	−0.0118	−0.0189	−0.0267	−0.0338	−0.0388
1000		−1.3e−006	−0.0001	−0.0007	−0.0026	−0.0062	−0.0118	−0.0189	−0.0267	−0.0338	−0.0388
5	Damping error (%)	−4.4e−006	−0.0004	−0.0029	−0.0103	−0.0247	−0.047	−0.0753	−0.1062	−0.1344	−0.1543
50		−3.5e−006	−0.0004	−0.0029	−0.0103	−0.0247	−0.047	−0.0753	−0.1062	−0.1344	−0.1543
100		−1.4e−006	−0.0004	−0.0029	−0.0103	−0.0247	−0.047	−0.0753	−0.1062	−0.1344	−0.1543
200		−7.1e−006	−0.0004	−0.0029	−0.0103	−0.0247	−0.047	−0.0753	−0.1062	−0.1344	−0.1543
300		−5.6e−006	−0.0004	−0.0029	−0.0103	−0.0247	−0.047	−0.0753	−0.1062	−0.1344	−0.1543
400		−3.6e−006	−0.0004	−0.0029	−0.0103	−0.0247	−0.047	−0.0753	−0.1062	−0.1344	−0.1543
500		−3.9e−006	−0.0004	−0.0029	−0.0103	−0.0247	−0.047	−0.0753	−0.1062	−0.1344	−0.1543
1000		−6.1e−006	−0.0004	−0.0029	−0.0103	−0.0247	−0.047	−0.0753	−0.1062	−0.1344	−0.1543
5	MAC	1	1	1	1	1	1	1	1	1	1
50		1	1	1	1	1	1	1	1	1	1
100		1	1	1	1	1	1	1	1	1	1
200		1	1	1	1	1	1	1	1	1	1
300		1	1	1	1	1	1	1	1	1	1
400		1	1	1	1	1	1	1	1	1	1
500		1	1	1	1	1	1	1	1	1	1
1000		1	1	1	1	1	1	1	1	1	1

Table 8 compares the prediction results from both the proportional and non-proportional models of MAFVRO algorithms. The predicted natural frequencies are very good within 2% errors. The damping ratio predictions are also good and can only be obtained by the non-proportional model. It is noted that the mode shape prediction is also good. The MAC matrix between the predicted and theoretical mode shape vectors revealed perfectly the unity matrix. The MAC value for each mode is shown to be 1 and indicates the good prediction for mode shapes.

Table 7
Effect of different numerical methods for different sensors on the predicted natural frequencies.

Type of sensor	Numerical method	f_s	f_s/f_6	ε_1	ε_2	ε_3	ε_4	ε_5	ε_6
Displacement sensors	1st Backward formula	7000	22.65	−0.14	−0.51	−0.72	−1.71	−1.89	−2.19
	2nd Backward formula	7800	25.24	0.03	0.27	0.70	1.21	1.67	2.05
	1st Central formula	5800	18.77	−0.03	−0.25	−0.64	−1.11	−1.55	−1.86
	2nd Central formula	**2200**	**7.12**	**0.00**	**−0.04**	**−0.23**	**−0.68**	**−1.30**	**−1.84**
Accelerometers	Mid-point rule	5500	17.80	−0.03	−0.28	−0.71	−1.23	−1.72	−2.06
	Trapezoid rule	7300	23.62	0.02	0.15	0.31	−0.18	−0.34	−0.09
	Simpson's rule	**3800**	**12.23**	**0.00**	**0.00**	**−0.02**	**−0.09**	**−0.76**	**−0.04**

Note: $N_k=200$, $k=50$, NR=0 (%).

Table 8
Comparison of proportional and non-proportional MAFVRO methods for a 3-dof system.

MAFVRO method	Response model	Predicted natural frequency (Hz)	Freq. error (%)	Predicted damping ratio (%)	Damping ratio error (%)	MAC
Proportional damping	Proportional damping	70.8267	−0.0056	–	–	1
		197.8059	−0.3311	–	–	1
		282.8160	−1.3847	–	–	1
	Non-proportional damping	70.8195	−0.0168	–	–	1
		197.7992	−0.3358	–	–	1
		282.7668	−1.3994	–	–	1
Non-proportional damping	Proportional damping	70.8267	−0.0056	0.2225	−0.0222	1
		197.8060	−0.3310	0.6154	−1.3034	1
		282.8178	−1.3841	0.8524	−5.3918	1
	Non-proportional damping	70.8275	−0.0056	0.2417	−0.0222	1
		197.8086	−0.3311	0.4299	−1.3035	1
		282.8089	−1.3848	0.1834	−5.3924	1

Note: $N_k=200$, $k=50$, $f_s=2200$ Hz, NR=0 (%).

Table 9
Effect of noise ratio (NR) for different damping models on the predicted natural frequency errors ε_r (%).

MAFVRO method	Response model	NR (%)	ε_1	ε_2	ε_3	ε_4	ε_5	ε_6	ε_7	ε_8	ε_9	ε_{10}
Proportional damping	Proportional damping	2	0.39	−0.10	0.26	0.09	0.15	−0.03	−0.41	−0.03	−0.49	**2.83**
	Non-proportional damping	3	0.23	0.57	0.40	0.54	0.35	0.29	0.75	1.11	1.10	**2.44**
Non-proportional damping	Proportional damping	1	0.10	−0.05	0.02	−0.06	−0.24	−0.47	−0.89	−1.13	**−1.13**	0.90
	Non-proportional damping	**3**	0.92	0.53	0.43	0.41	0.08	−0.14	−0.39	−0.48	−0.36	**2.30**

Note: $N_k=200$, $k=50$, $f_s=2200$ Hz.

Table 9 shows the simulation results for considering the measurement noise effects in using displacement sensors for different combinations of MAFVRO models and response simulation models. The maximum predicted natural frequency errors are limited to about 2%, and the maximum tolerant NR is shown for each case study. For the 10-dof system, the maximum tolerable NR is about 3% for the non-proportional MAFVRO model, when the non-proportional response model is adopted. The predictions for damping ratios and mode shapes, which are not shown for brevity, are generally good and similar to those results shown in Table 8 for the natural frequency errors within 2%.

Table 10 reveals the maximum tolerable NR values in MAFVRO applications for using different sensors by the non-proportional MAFVRO model. In general, the MAFVRO algorithm can accommodate higher NR values for fewer dofs system. For example, the use of displacement sensors can tolerate up to 11% NR for the 3-dof system, while there is only 3% NR for the 10-dof system. NR values are much smaller for the accelerometer application due to twice of numerical operations in simulations. One is the numerical differential operation on the displacement data to obtain the velocity and acceleration responses, and another is the numerical integration operation on the acceleration data to obtain the velocity and displacement in the MAFVRO algorithm. If the theoretical response of $\mathbf{x}$, $\dot{\mathbf{x}}$ and $\ddot{\mathbf{x}}$ is used for simulating the use of accelerometers to avoid the accumulated numerical errors, the accommodated NR (%) values will be the same for both displacement sensors and accelerometers, since the formulated system response matrices are exactly the same. In that

Table 10
Effect of different dofs on the tolerable noise ratio (NR) for different sensors on the predicted natural frequency errors ε_r (%).

dofs	NR (%)	ε_1	ε_2	ε_3	ε_4	ε_5	ε_6	ε_7	ε_8	ε_9	ε_{10}	ε_{avg}	ε_{max}	ε_{min}
(a) Displacement sensors														
3	11	1.8490	0.6722	−0.2340								0.7624	1.8490	−0.2340
4	10	1.8780	2.5759	2.3880	1.5380							2.0950	2.5759	1.5380
5	8	2.0301	2.1215	1.3691	1.7045	0.8210						1.8092	2.1215	1.3691
6	6	1.0404	0.8151	1.4491	0.8207	−0.4929	−0.3446					0.5480	1.4491	−0.4929
7	5	0.7223	0.8260	0.4686	0.9278	0.0109	0.6722	2.0950				0.8175	2.0950	0.0109
8	3.5	0.6034	0.6353	0.4362	0.5213	0.0101	−0.3296	−0.3192	1.2742			0.3540	1.2742	−0.3296
9	3	0.8443	0.4097	0.3037	0.3078	0.2141	−0.2897	−0.4270	−0.0460	1.6823		0.3332	1.6823	−0.4270
10	3	0.4137	0.2757	0.2164	0.3788	0.1343	−0.2918	−0.2148	−0.8591	−0.7105	1.2498	0.0592	1.2498	−0.8591
(b) Accelerometers														
3	0.4	0.2306	−1.0519	−0.1432								−0.3215	0.2306	−1.0519
4	0.3	0.0522	−1.3762	−1.9140	−1.0772							−1.0788	0.0522	−1.9140
5	0.2	−0.0534	0.0642	−0.0235	−1.9117	−2.1502						−0.8149	0.0642	−2.1502
6	0.2	−0.1298	0.1270	−1.2698	−0.1445	−4.5543	−0.3863					−1.0596	0.1270	−4.5543
7	0.1	0.5307	−0.1260	−0.1004	−0.3213	−0.1223	−0.2114	−0.8695				−0.1743	0.5307	−0.8695
8	0.1	0.0671	0.0171	−0.0119	0.0185	0.0104	−0.0440	−0.4303	−0.5533			−0.1158	0.0671	−0.5533
9	0.1	0.0192	−0.0004	−0.0051	−0.0018	0.0296	−0.0082	0.0043	−0.0839	−0.2031		−0.0277	0.0296	−0.2031
10	0.04	−0.1166	0.0214	−0.0052	−0.0360	0.0132	0.0074	−0.0115	0.0044	−0.0688	−0.6710	−0.0863	0.0214	−0.6710

Note: for (a): $N_k = 200$, $k = 50$, $f_s = 2200$ Hz, NR=0 (%); for (b): $N_k = 200$, $k = 50$, $f_s = 3800$ Hz, NR=0 (%).
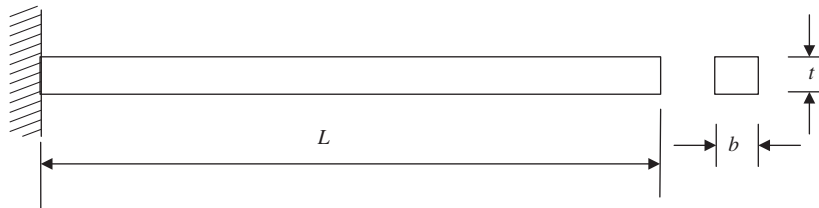
Fig. 4. Cantilever beam diagram.

Table 11
Physical properties of the cantilever beam.

Physical properties	Cantilever beam
Young's modulus (E)	191×10^9 N/m^2
Poisson ratio (ν)	0.32
density (ρ)	8791 kg/m^3
Length (L)	0.3 m
Width (b)	0.04 m
Height (t)	0.002 m

case, the results in Table 10(b) will become the same as Table 10(a). Here, Table 10(b) is shown to reveal the effect of the accumulated numerical errors.
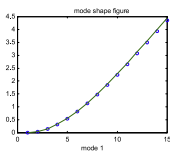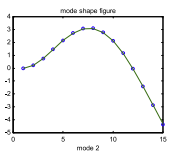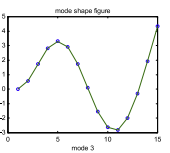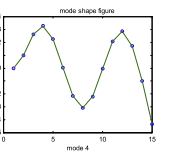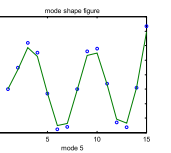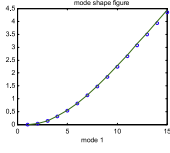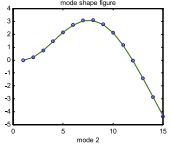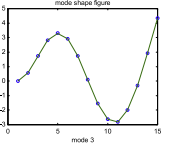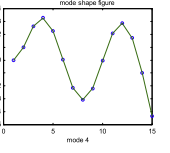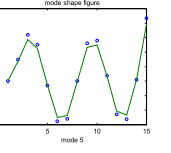
In summary, the use of the developed MAFVRO algorithms in the mdof system application is feasible. The non-proportional viscous damping model for the MAFVRO algorithm developed in this work is also shown to obtain the natural frequencies, damping ratios and mode shape vectors, simultaneously, from the free vibration response only without the prior knowledge of system matrices.

5.2. Beam structure application

A steel cantilever beam is considered. Fig. 4 shows the illustration of the beam structure and Table 11 reveals its physical properties. The proportional viscous damping model for the beam is adopted as formulated by Wang [24] that showed the derivation of modal analysis and transient response analysis. The beam lateral displacement response due to the initial conditions is simulated and used as the measured data to be applied to the developed MAFVRO algorithms for both the proportional and non-proportional models. It is noted that the lateral displacement response can be obtained with the exact solutions for free vibration analysis under the thin beam assumptions. The velocity and acceleration of the beam are determined by the second-order central formula as shown in Table 1.
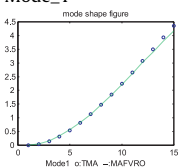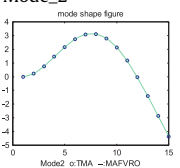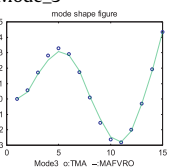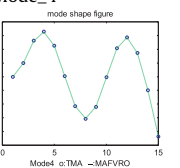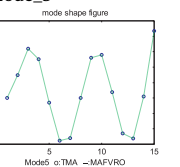
Table 12
Modal parameter prediction results for the cantilever beam by the proportional damping model of MAFVRO.
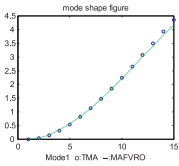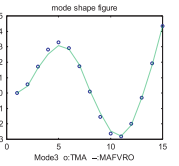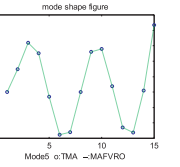
(a) Displacement sensors

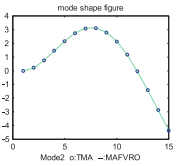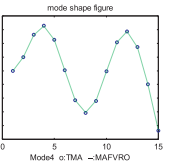**Predicted natural frequencies**

Mode	1	2	3	4	5
TMA	16.733	104.86	293.62	575.37	951.13
MAFVRO	16.747	104.86	293.60	575.03	947.16
Err (%)	**0.083597**	**0.0000**	**−0.00681**	**−0.05913**	**−0.41915**

MAC values

MAFVRO	TMA Mode_1	Mode_2	Mode_3	Mode_4	Mode_5
Mode_1	**1.0000**	0.0176	0.0186	0.0199	0.0208
Mode_2	0.0176	**1.0000**	0.0198	0.0210	0.0221
Mode_3	0.0187	0.0199	**1.0000**	0.0221	0.0232
Mode_4	0.0198	0.0210	0.0221	**1.0000**	0.0243
Mode_5	0.0210	0.0247	0.0234	0.0234	**0.9999**

Mode shape comparison

Mode_1	Mode_2	Mode_3	Mode_4	Mode_5

(b) Accelerometers

Predicted natural frequencies

Mode	1	2	3	4	5
TMA	16.733	104.86	293.62	575.37	951.13
MAFVRO	16.738	107.06	297.81	584.04	971.71
Err (%)	**0.0298**	**2.0549**	**1.4069**	**1.4844**	**2.1179**

MAC values

MAFVRO	TMA Mode_1	Mode_2	Mode_3	Mode_4	Mode_5
Mode_1	**0.9998**	0.0143	0.0181	0.0182	0.0202
Mode_2	0.0174	**1.0000**	0.0197	0.0193	0.0219
Mode_3	0.0202	0.0180	**0.9973**	0.0375	0.0252
Mode_4	0.0198	0.0210	0.0222	**1.0000**	0.0245
Mode_5	0.0192	0.0176	0.0218	0.0016	**0.9591**

Mode shape comparison

Mode_1	Mode_2	Mode_3	Mode_4	Mode_5

Note: $N_k = 100$, $k = 50$, $f_s = 8000$ Hz, NR $= 0$ (%).

By applying the developed MAFVRO algorithms to the beam structure, the free vibration response of the beam should be measured at a number of points over the beam. In this study, there are 14 points along the beam length, i.e. $m = 14$. Therefore, the number of dofs becomes $n = m$. Tables 12(a) and (b) show the prediction results via the proportional model of MAFVRO algorithm by using displacement sensors and accelerometers, respectively. Both the natural frequency and mode shape predictions are very good for the first five modes. For the use of displacement sensors Table 12(a) reveals the natural frequency prediction errors are less than 1%, while Table 12(b) for the use of accelerometers results in about 2%

Table 13
Modal parameter prediction results for the cantilever beam by the non-proportional damping model of MAFVRO.

(a) Displacement sensors

Predicted natural frequencies

Mode	1	2	3	4	5
TMA	16.733	104.86	293.62	575.37	951.13
MAFVRO	16.730	104.86	293.60	575.03	947.05
Err (%)	−0.017	0.0000	−0.0068	−0.059	−0.4308

Predicted modal damping ratios

Mode	1	2	3	4	5
TMA	0.00047	0.000075	0.000027	0.000013	0.0000083
MAFVRO	0.00056	0.000075	0.000020	0.000013	0.0001073
Err (%)	15	−0.78	−30	−0.47	92.2

MAC values

	TMA				
MAFVRO	Mode_1	Mode_2	Mode_3	Mode_4	Mode_5
Mode_1	1.0000	0.0176	0.0186	0.0199	0.0208
Mode_2	0.0176	1.0000	0.0198	0.0210	0.0221
Mode_3	0.0187	0.0199	1.0000	0.0221	0.0232
Mode_4	0.0198	0.0210	0.0221	1.0000	0.0243
Mode_5	0.0209	0.0219	0.0229	0.0242	0.9999

Mode shape comparison

(b) Accelerometers

Predicted natural frequencies

Mode	1	2	3	4	5
TMA	16.733	104.86	293.62	575.37	951.13
MAFVRO	16.712	106.23	297.55	584.27	969.84
Err (%)	−0.1256	1.2896	1.3207	1.52326	1.92918

Predicted modal damping ratios

Mode	1	2	3	4	5
TMA	0.00047	0.000075	0.000027	0.000013	0.0000083
MAFVRO	0.00705	0.000280	0.000014	0.000030	0.0016630
Err (%)	93.2580	72.8758	−83.15312	54.81394	99.49678

MAC values

	TMA				
MAFVRO	Mode_1	Mode_2	Mode_3	Mode_4	Mode_5
Mode_1	0.9991	0.0145	0.0179	0.0182	0.0201
Mode_2	0.0177	1.0000	0.0198	0.0209	0.0221
Mode_3	0.0187	0.0198	1.0000	0.0224	0.0233
Mode_4	0.0198	0.0210	0.0221	1.0000	0.0243
Mode_5	0.0202	0.0208	0.0240	0.0234	0.9988

Mode shape comparison

Note: $N_k = 100$, $k = 50$, $f_s = 8000$ Hz, NR = 0 (%).

error. The slightly higher errors in using accelerometers are the result of accumulated numerical errors from the differentiation and integration process in simulating the beam transient responses to formulate the system response matrices for the MAFVRO application. The MAC matrices between the predicted and theoretical mode shapes are nearly close to the unity matrices, i.e. the mode shapes show good comparisons and possess the orthogonal properties. The modal parameters predictions are very good.

For the modal parameter prediction results from the non-proportional MAFVRO model as shown in Table 13(a) and (b) by using displacement sensors and accelerometers, respectively, both natural frequencies and mode shapes also reveal very good predictions, while the damping ratios may reveal high errors but in the reasonable range. Note that the damping errors in Table 13(b) for the accelerometer application are larger than those in Table 13(a) for the displacement sensor is due to the numerical operation in obtaining the simulated acceleration response as discussed in Table 10 for mdof systems. The presented MAFVRO algorithm shows an effective way to obtain the modal parameters from the free vibration response only without the prior knowledge of system matrices. Feeny and Liang [25] expanded the POD method [23] to the discrete and continuous systems in random excitation; however, the requirement for a prior knowledge of the mass matrix is its limitation. The MAFVRO algorithms for both proportional and non-proportional viscous damping models are simple and straightforward as revealed in this work. In particular, the MAFVRO methods require no prior knowledge of system matrices and only the free vibration transient response in determining the structural modal parameters.

6. Conclusions

This paper extends the proportional viscous damping model of the MAFVRO algorithm [20] to the non-proportional model. Additionally, the formulation for the use of accelerometers other than the displacement sensors is provided. The MAFVRO algorithm development is theoretically complete. The case studies for mdof systems and the beam structure are demonstrated by simulation results. Results show that the modal data for both the discrete and continuous systems can be well identified by the MAFVRO algorithms. The developed modal analysis methods from the free vibration response only are promising and have the potential for practical applications. For the proportional damping model, the normal mode analysis is assumed and thus only the natural frequencies and mode shapes can be obtained. The predicted mode shape vector is real. For the non-proportional damping model, the complex mode analysis is adopted. The modal damping ratios can also be obtained in addition to the natural frequencies and mode shapes. In particular, the mode shape vector is complex and more appropriate for practical structures. This work enhances the modal analysis technique by using the free vibration response only and shows the feasibility of the MAFVRO in practical applications for both the discrete and continuous systems.

Acknowledgements

References

[1] D.J. Ewins, *Modal Testing: Theory and Practice*, Second Edition, Research Studies Press Ltd, Letchworth, Hertfordshire, England, 2000.
[2] K.G. McConnell, *Vibration Testing Theory and Practice*, John Wiley & Sons, Inc., New York, 1995.
[3] B.T. Wang, Structural modal testing with the use of various forms of actuators and sensors, *Mechanical Systems and Signal Processing* 12 (1998) 627–639.
[4] R. Brincker, L.M. Zhang, P. Andersen, Modal identification from ambient responses using frequency domain decomposition. *Proceedings of 18th International Modal Analysis Conference (IMAC)*, San Antonio, TX, USA, 2000, pp. 625–630.
[5] R. Brincker, C.E. Ventura, P. Andersen, Damping estimation by frequency domain decomposition. *Proceedings of 19th International Modal Analysis Conference (IMAC)*, Orlando, FL, USA, 2001, pp. 441–446.
[6] B. Cauberghe, P. Guillaume, P. Verboven, E. Parloo, Identification of modal parameters including unmeasured forces and transient effects, *Journal of Sound and Vibration* 265 (2003) 609–625.
[7] F. Magalhaes, A. Cunha, E. Caetano, R. Brincker, Damping estimation using free decays and ambient vibration tests, *Mechanical Systems and Signal Processing* doi:10.1016/j.ymssp.2009.02.011.
[8] C. Gentile, N. Gallino, Ambient vibration testing and structural evaluation of an historic suspension footbridge, *Advances in Engineering Software* 39 (2008) 356–366.
[9] S.M. Moore, J.C.S. Lai, K. Shankar, ARMAX modal parameter identification in the presence of unmeasured excitation—II: numerical and experimental verification, *Mechanical Systems and Signal Processing* 21 (2007) 1616–1641.
[10] N. Larbi, J. Lardies, Experimental modal analysis of a structure excited by a random force, *Mechanical Systems and Signal Processing* 14 (2) (2000) 181–192.
[11] V. Papakos, S.D. Fassois, Multichannel identification of aircraft skeleton structures under unobservable excitation: a vector AR/ARMA framework, *Mechanical Systems and Signal Processing* 17 (6) (2003) 1271–1290.
[12] C. Devriendt, P. Guillaume, The use of transmissibility measurements in output-only modal analysis, *Mechanical Systems and Signal Processing* 21 (2007) 2689–2696.
[13] C. Devriendt, P. Guillaume, Identification of modal parameters from transmissibility measurements, *Journal of Sound and Vibration* 314 (2008) 343–356.
[14] E. Parloo, P. Verboven, P. Guillaume, M. Van Overmeire, Sensitivity-based mass-normalization of mode shape estimates from output-only data, *Proceedings of the International Conference on Structural System Identification*, Kassel, Germany, 2001, pp. 627–636.

[15] E. Parloo, P. Verboven, P. Guillaume, M. Van Overmeire, Force identification by means of in-operation modal models, *Journal of Sound and Vibration* 262 (2003) 161–173.

[16] M. Abdelghani, M. Goursat, T. Biolchini, On-line modal monitoring of aircraft structures under unknown excitation, *Mechanical Systems and Signal Processing* 13 (6) (1999) 839–853.

[17] S. Naylor, J.E. Cooper, J.R. Wright, Modal parameter estimation of non-proportionally damped systems using force appropriation, *Proceedings of the IMAC-XV, International Modal Analysis Conference*, Orlando, FL, 1997.

[18] C.S. Huang, W.C. Su, Identification of modal parameters of a time invariant linear system by continuous wavelet transformation, *Mechanical Systems and Signal Processing* 21 (2007) 1642–1664.

[19] J. Lardies, Modal parameter identification from output-only measurements, *Mechanics Research Communication* 24 (5) (1997) 521–528.

[20] B.T. Wang, D.K. Cheng, Modal analysis of mdof system by using free vibration response data only, *Journal of Sound and Vibration* 311 (3–5) (2008) 737–755.

[21] W. Zhou, D. Chelidze, A new method for vibration modal analysis, *Proceeding of the SEM Annual Conference and Exposition on Experimental and Applied Mechanics*, Portland, OR, USA, 2005, pp. 390–391.

[22] B.F. Feeny, R. Kappagantu, On the physical interpretation of proper orthogonal modes in vibration, *Journal of Sound and Vibration* 211 (1998) 607–616.

[23] S. Han, B. Feeny, Application of proper orthogonal decomposition to structural vibration analysis, *Mechanical System and Signal Processing* 17 (2003) 989–1001.

[24] B.T. Wang, Vibration analysis of a continuous system subject to generic forms of actuation forces and sensing devices, *Journal of Sound and Vibration* 319 (2009) 1222–1251.

[25] B.F. Feeny, Y. Liang, Interpreting proper orthogonal modes of randomly excited vibration system, *Journal of Sound and Vibration* 265 (2003) 953–966.